

## A study of the electric field transient at the Au/semi-insulating GaAs contact under an alternating current square-pulse bias

This article has been downloaded from IOPscience. Please scroll down to see the full text article.

2002 J. Phys.: Condens. Matter 14 13705

(<http://iopscience.iop.org/0953-8984/14/49/325>)

View [the table of contents for this issue](#), or go to the [journal homepage](#) for more

Download details:

IP Address: 171.66.16.97

The article was downloaded on 18/05/2010 at 19:21

Please note that [terms and conditions apply](#).

# A study of the electric field transient at the Au/semi-insulating GaAs contact under an alternating current square-pulse bias

C C Ling<sup>1,3</sup>, S Fung<sup>1</sup>, C D Beling<sup>1</sup>, Y Y Shan<sup>1</sup> and A H Deng<sup>2</sup>

<sup>1</sup> Department of Physics, The University of Hong Kong, Pokfulam Road, Hong Kong, People's Republic of China

<sup>2</sup> Department of Applied Physics, Sichuan University, Chengdu, Sichuan 610065, People's Republic of China

E-mail: ccling@hku.hk

Received 7 August 2002

Published 29 November 2002

Online at [stacks.iop.org/JPhysCM/14/13705](http://stacks.iop.org/JPhysCM/14/13705)

## Abstract

Positron lifetime spectroscopy combined with a 50 V AC applied square-wave bias has been used to probe the electric field in the 2  $\mu\text{m}$  region next to an Au/SI-GaAs contact. The electric fields spatially and time averaged over the reverse half-period at different temperatures (255–295 K) and pulsing periods ( $\sim 1$  ms–10  $\mu\text{s}$ ) have been obtained using a numerical differentiation technique. It is found that within the temperature range studied, the electric field first increases as a function of time to a maximum of about 10  $\text{kV cm}^{-1}$  and then decreases, before finally saturating at the DC value of 7  $\text{kV cm}^{-1}$ . The increase of the electric field with time is attributed as previously to the electron emission from the EL2 defect. The subsequent electric field decrease is associated with the onset of a thermally activated process with an energy barrier of  $1.03 \pm 0.15$  eV. This process, which causes the neutralization of the space charge region, may be tentatively attributed to the recombination centres EL5 or EL6.

## 1. Introduction

Besides their use as a vacancy probe in semiconductors [1–3], different techniques in positron annihilation spectroscopy (PAS) have also been employed to reveal the internal electric field at buried internal interfaces [4–8]. In the case of the metal–semiconductor contact, positrons implanted into the sample can drift back to the interface under the action of an internal electric field, get trapped by voids at the interface, and annihilate from these open volume defect sites. If such circumstances arise, as they do in the case of the metal/SI-GaAs interface, positrons annihilating from the interfacial defect state exhibit a longer lifetime as compared to the bulk

<sup>3</sup> Author to whom any correspondence should be addressed.

state. By monitoring the interfacial lifetime component, the mean electric field within the space charge region can be deduced. Ling *et al* [4] and Shek *et al* [5] have employed this technique to probe the electric field at the DC-biased metal/SI-GaAs contact using a derived relation between the observed interfacial component intensity and the electric field profile.

The electric field at the metal/SI-GaAs Schottky contact under DC bias has been investigated by various methods [4–6, 9–11] with fairly consistent results. The depletion approximation was found to fail to give a good representation of the electric field structure at the contact. It is now understood that with the application of a reverse DC bias, a high-field region with a constant field strength ( $\sim 10 \text{ kV cm}^{-1}$ ) is formed which extends well into the SI-GaAs bulk, falling abruptly after having extended to the depth commensurate with the applied bias. The constancy of the electric field has been attributed to the enhancement of the electron capture cross-section of the deep donor EL2 [9–11]. Direct observation of enhancement of the EL2 capture cross-section at high electric field ( $\sim 10 \text{ kV cm}^{-1}$ ) was reported by Prints and Parsey [12], and by Prinz and Rechkunov [13]. As the electron–phonon coupling of EL2 is strong, there is a large Frank–Condon shift in the ionization process  $\text{EL2}^0 \rightarrow \text{EL2}^+$ . The electron capture of  $\text{EL2}^+$  thus involves the crossing of an energy barrier  $\varepsilon_b \sim 70 \text{ meV}$ , followed by the multiphonon emission process [14, 15]. Under low-electric-field conditions, the capture cross-section for the transition  $\text{EL2}^+ + e^- \rightarrow \text{EL2}^0$  is thus temperature dependent and varies as  $\exp(-\varepsilon_b/kT)$ . The high-field enhancement of the EL2 capture cross-section begins to occur at  $E \sim 10 \text{ kV cm}^{-1}$  and is related to the process in which hot electrons accelerated by the electric field have a higher probability of crossing the barrier  $\varepsilon_b$  for the multiphonon emission process [16].

Shan *et al* [17] performed positron lifetime measurements on an AC square-wave-biased Au/SI-GaAs system in the frequency range 1 mHz–1 kHz. The effect of the AC bias was to sequentially reverse and zero bias the metal/SI-GaAs junction. Under the assumption of the depletion approximation (i.e. a space charge region being formed next to the Schottky contact by the complete ionization of a donor defect), Shan *et al* [17] showed how the observation could be explained by a model involving electron emission from, and capture into, the deep-level donor EL2. The result demonstrated the feasibility of employing this technique to study the thermal emission from deep-level defects. Unlike in conventional DLTS, where the thermal transient of a deep level is monitored by the capacitance of a junction, it has been shown that space charge transients can also be revealed by monitoring the transient behaviour of the interfacial long-lifetime-component intensity [18].

The depletion approximation had originally been assumed in interpreting the data of [17]. This should necessarily be some cause for concern, as it has been generally accepted that it is not a valid approximation for the case of metal/SI-GaAs contact [4–6, 9–11]. This study aims at rectifying this inconsistency by taking a fresh look at the data already presented in [18]. A novel analysis technique that involves differentiation of the primary data is given which more clearly reveals the electric field transient at the metal–SI-GaAs interface. Moreover, this technique is based on a more correct description of the spatial distribution of the electric field at the interface. The extracted EL2 ionization energy is only slightly different from [17]. Moreover, the new method of analysis permits the high-field neutralization of  $\text{EL2}^+$  to be clearly seen and analysed.

## 2. Experimental details

As already mentioned, the data used in the present work are those given in [18]; the reader is referred to that paper for full experimental details. Briefly, however, two Au/SI-GaAs junctions were placed in a back-to-back configuration, with a  $5 \mu\text{Ci } ^{22}\text{Na}$  source sandwiched between

them. A 50 V amplitude square-wave bias was applied to the assembly in such a way that when under reverse bias the electric fields in both samples were directed towards the positron source and the Au/SI-GaAs interfaces. Positron lifetime spectra were taken during the reverse biasing, and both the temperature and frequency of the bias were varied. Implanted positrons drifted back towards the positron implanting contacts under the influence of the internal electric field. A fraction of these positrons arrived at the metal–semiconductor interface, got trapped into the interfacial state, and annihilated there. The intensity of the interfacial lifetime component of the positron lifetime spectrum was thus related to the internal electric field and could be used to monitor the field strength if the positron drift–annihilation equation was solved.

Analysing with the program POSITRONFIT [19], the lifetime spectra were in all cases found to be well represented by a two-exponential-component fit. In particular, the long-lifetime component  $\tau_2$  observed for all the spectra was found to be constant at about 400 ps and was, as previously, attributed to positrons annihilating at voids at the Au/SI-GaAs interface [4, 5]. The interfacial intensity  $I_2$  (i.e. the intensity of the  $\tau_2$ -component) is related to the fraction of positrons annihilating at the interface, and thus depends on the strength of the electric field at the Schottky contact that causes the drift of the implanted positrons back to the interface. The interfacial intensity  $I_2$  (figure 1 of [18]) is found to asymptotically approach the DC value of  $\sim 8.5\%$  at low frequency. It rises to a peak intensity of  $\sim 12.5\%$  at some intermediate frequency and thereafter drops to  $\sim 7\%$  at higher frequencies ( $\sim 10$ – $100$  Hz). The location of the peak depends on the sample temperature, shifting to higher frequencies at higher temperatures.

### 3. Results and analysis

Shek *et al* [5] have constructed a drift–annihilation model to describe the positron dynamics of a radioactive source implanting positrons under the influence of an arbitrary electric field profile  $E(x)$ . The electric field profile was modelled by an  $N$ -layer structure, in which the electric field is taken to be constant within each layer, and the positron implantation profile was taken to be  $p(x) = \alpha \exp(-\alpha x)$  [20, 21]. The intensity of the interfacial lifetime component found in the lifetime spectrum was solved analytically. The relation between the spatially average effective field and the measured interfacial lifetime component  $I_2$  was given as [5]

$$\langle E \rangle_x = \frac{\lambda_b - \lambda_2}{\alpha \mu_+} \frac{I_2}{1 - I_2} \quad (1)$$

where  $\mu_+$  is the positron mobility and  $\lambda_b$  and  $\lambda_2$  are the rates of annihilation of the bulk and interfacial states respectively. The criterion for equation (1) to be a good estimate is that the electric field has to be fairly constant over the region of positron drift. This turns out to be a good approximation in the case of the metal/SI-GaAs interface. The distance over which positrons will drift at the reverse-biased junction  $\mu_+ E \tau_b$  can be estimated to be  $\sim 2 \mu\text{m}$  by taking the DC interfacial electric field  $E \sim 10 \text{ kV cm}^{-1}$  [9–11],  $\mu_+ \sim 100 \text{ cm}^2 \text{ V}^{-1} \text{ s}^{-1}$  [4–6], and the GaAs bulk lifetime  $\tau_b \sim 230 \text{ ps}$  [2, 3]. Thus in making measurement of the electric field via  $I_2$  under reverse bias, the interface electric field is being sensed out to a few microns depth, since it is known that the electric field is effectively constant to tens of microns under reverse bias [10, 11] and equation (1) is considered a good approximation.

With the raw lifetime data already presented in [18], the effective electric field  $E_{eff}$  in the reverse half-period was obtained from the definition

$$E_{eff} = \frac{\lambda_b - \lambda_2}{\alpha \mu_+} \frac{\langle I_2 \rangle_t}{1 - \langle I_2 \rangle_t} \quad (2)$$

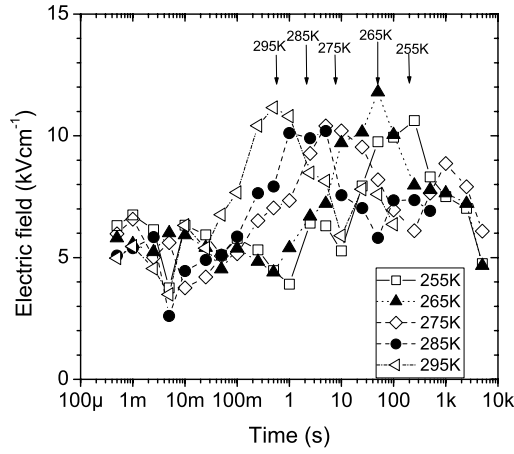


**Figure 1.** The electric field transient in the reverse-bias half-period at different temperatures. The time axis has a log scale and the lines joining the data points are only for visual guidance. The peak positions at different temperatures are indicated by arrows.

where  $\langle I_2 \rangle_t$  is the time average of  $I_2(t)$  in the reverse half-period and thus the effective measured value in the present experiment. If  $I_2$  is much smaller than unity, then the time average of  $\langle E \rangle_x$  in equation (1) over the reverse-biased half-period is approximately equal to  $E_{eff}$ , i.e.,

$$E_{eff}(T) = \frac{2}{T} \int_0^{T/2} \langle E \rangle_x(t) dt. \quad (3)$$

The effective electric field  $E_{eff}(T)$  is a function of the period, but is not the direct electric field transient  $\langle E \rangle_x(t)$  (i.e. the spatially averaged electric field close to the contact as a function of time) in the reverse half-period. However, the electric field transient  $\langle E \rangle_x(t)$  can be obtained by differentiating equation (3), from which it is found that

$$\langle E \rangle_x(t) = [E_{eff}(T)]_{T=2t} + \left[ T \frac{dE_{eff}(T)}{dT} \right]_{T=2t}. \quad (4)$$

The electric field transients  $\langle E \rangle_x(t)$  as obtained from equations (2) and (4) for temperatures ranging from  $T = 255$  to  $295$  K are shown in figure 1. At all temperatures,  $\langle E \rangle_x(t)$  increases with respect to time from about  $5 \text{ kV cm}^{-1}$ , reaches a maximum of about  $10 \text{ kV cm}^{-1}$ , and thereafter drops to the DC limit of  $\sim 7 \text{ kV cm}^{-1}$ . In order to provide a clearer view of the rising part of the electric field transient, figure 2 was plotted, which shows the electric field data at different temperatures against different timescales. As the temperature increases, it is seen that the time required for the electric field to reach the maximum shifts from of the order of  $\sim 100$  s at  $255$  K to  $\sim 1$  s at  $295$  K.

### 3.1. Thermal electron emission from the deep-level donor EL2

As noted in earlier works [17, 18], the increase of electric field with respect to time (or, in [17, 18], the increase of  $I_2$  with increasing period) and the peak shift in figure 1 can easily be explained in terms of the thermal electron emission from the deep-level defect EL2. When the contact is in the reverse-bias half-period, the deep-level defects close to the contact start emitting electrons and become ionized ( $\text{EL2}^0 \rightarrow \text{EL2}^+ + e^-$ ). This increases the electric field close to the contact and consequently the interfacial intensity  $I_2$  increases. The profile of the electric field transient  $\langle E \rangle_x(t)$  shifting to smaller time values as the temperature increases

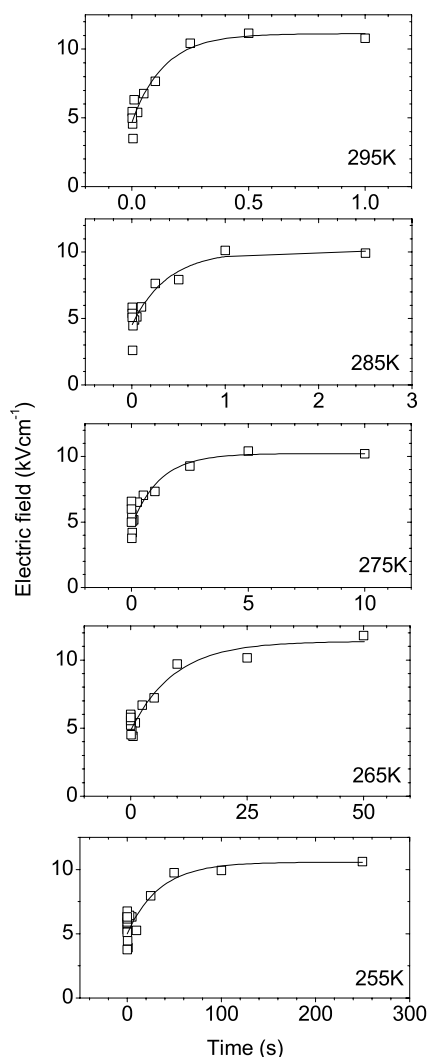


**Figure 2.** The rising parts of the electric field transients at different temperatures. The transients are plotted with different timescales. The solid curves are fitted by the model involving electron emission from the deep level EL2.

thus results from the thermal emission rate of the deep-level defect increasing with increasing temperature. However, a more careful consideration of the cause of the peak is required, since the deep-donor ionization on its own would only give rise to a continued monotonic increase in  $\langle E \rangle_x(t)$ .

The electric field profile of the DC reverse-biased metal/SI-GaAs contact has been studied by different methods and similar results have been obtained [4–6, 9–11]. In contrast to the prediction of the commonly used depletion approximation, at a fixed applied bias, the electric field profile consists of a high-field region close to the contact extending from  $x = 0$  to  $x_0$ , and the electric field inside the high-field region is approximately constant for a fixed bias voltage. The value of  $x_0$  varies from  $10 \mu\text{m}$  (zero bias) to  $200 \mu\text{m}$  (bias  $\sim 240 \text{ V}$ ), according to the applied bias. The electric field then drops abruptly to a low value  $E_{bulk}$  within a narrow

region  $d \sim 20 \mu\text{m}$  [11]. This implies that the space charge density function is close to zero for  $0 < x < x_0$ , and is box-shaped in the region  $x_0 < x < x_0 + d$ . For high applied bias, the electric field must first strengthen close to the contact until its field reaches a critical value  $E_C \sim 10 \text{ kV cm}^{-1}$ . As the electric field in the high-field region reaches  $E_C$ , the electric field value saturates. However, the width of the high-field region keeps on increasing so as to continue to obey the equation  $V = \int E dx$ . The clamping of the electric field value within the high-field region has been explained by the electric field enhancement of the EL2 capture cross-section [9–11].

As the applied bias varies between 0 and 50 V in the present study (which corresponds to values of  $x_0$  equal to about 10 and 50  $\mu\text{m}$  respectively [11]), the high-field region thus always has a width significantly larger than the sensitive region of the positron probe ( $\sim 2 \mu\text{m}$ ). This implies that the present measured  $\langle E \rangle_x(t)$  gives a good representation of the field strength of the high-field region. In order to model the electric field transient, at any time  $t$ , we consider a spatially constant electric field  $E_0(t)$  over the whole high-field region  $0 < x < x_0$ , and a box-shaped charge density (i.e. a spatially constant charge density  $N_+(t)$ ) over the abrupt falling region  $x_0 < x < x_0 + d$ . Poisson's equation in the region  $x_0 < x < x_0 + d$  then gives

$$E = E_{bulk} + \frac{ed}{\epsilon} N_+, \quad (5)$$

where  $E_{bulk}$  is the electric field in the bulk SI-GaAs that has not been subject to ionization. The rate of change of the ionized donor concentration is given by

$$dN_+/dt = e_n(N_0 - N_+) - c_n(E)N_+ \quad (6)$$

where  $e_n$  is the emission rate,  $c_n$  is the field-dependent capture rate, and  $N_0$  is the concentration of the deep donors. With the approximation that is commonly assumed in DLTS analysis, the capture term in equation (6) can be neglected in the emission half-period and thus equation (5) becomes

$$E = E_{bulk} + \frac{edfN_0}{\epsilon}(1 - e^{-e_n t}), \quad (7)$$

where  $f$  is the fraction of EL2 being ionized as  $t \rightarrow \infty$ . The value of  $f$  is smaller than unity because of the high-field-enhanced EL2 capture cross-section.

If we assume a constant width of the abruptly falling region  $d$ , which is about 20  $\mu\text{m}$  as seen in [11], the increase of the electric field with respect to time before reaching the maximum measured at different temperatures shown in figure 2 can be fitted with equation (7). The fitted curves are shown in figure 2 and reasonably represent the experimental data. The fitted value of the term  $edfN_0/\epsilon$  in equation (7) was found to be temperature independent. It is worth pointing out that  $fN_0$  is indeed the ionized EL2 concentration at the final steady state (or the DC limit at  $t \rightarrow \infty$ ), and the fitting yields a value of  $fN_0 = 2.15 \pm 0.19 \times 10^{13} \text{ cm}^{-3}$  if  $d$  is taken to be  $d \sim 20 \mu\text{m}$ . This value is consistent with the net ionized charge density of the box-shaped charge region ( $\sim 2 \times 10^{13} \text{ cm}^{-3}$ ) measured with the surface potential method [11]. As for the present sample, the concentration of EL2 is  $1.5 \times 10^{16} \text{ cm}^{-3}$ . This implies that only a fraction of about  $10^{-3}$  of the EL2 are ionized at the final state. The incomplete EL2 ionization is indeed a consequence of the high-field enhancement of the EL2 capture cross-section. The fitted values of  $e_n$  at different temperatures are shown as the Arrhenius plot in figure 3. The emission rate is given by [22]

$$e_n = \sigma_{n0}v_{n0}N_{C0}(T/T_0)^2 \exp(-E_a/kT). \quad (8)$$

$\sigma_{n0}$ ,  $v_{n0}$ , and  $N_{C0}$  are the defect capture cross-section, carrier velocity, and conduction band density of states at temperature  $T_0$  respectively; the observed straight-line behaviour is as expected. The Arrhenius plot gives the activation energy  $E_a$  of EL2 as  $0.88 \pm 0.07 \text{ eV}$ .

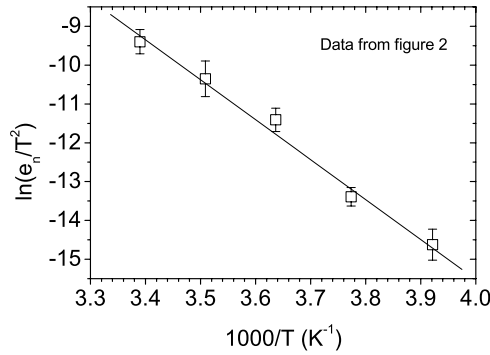


**Figure 3.** An Arrhenius plot of the thermally activated electron emission from EL2, which contributes to the increase of the electric field with respect to time seen in figure 2.

### 3.2. Neutralization of space charge

In the last section, electron emission from EL2 was discussed, which led to an increase of the interfacial electric field as a function of temperature and pulsing period. However, as shown in figure 1, irrespective of temperature, the measured electric field decreases as a function of time after reaching a maximum value of about  $10 \text{ kV cm}^{-1}$ . Such peaking behaviour requires some explanation. Shan *et al* [17] explained the observed  $I_2$  as a function of the pulsing period. Using the depletion approximation model, the fall in the observed  $I_2$  at large half-periods was attributed to the result of time variations in the overlapping of the depletion region and the positron implantation profile. Under reverse bias, on the depletion approximation, the depletion width ( $=\sqrt{2\varepsilon V/N_+}$ ) decreases with time. The depletion width at the 115 V applied reverse bias (which was the magnitude of the AC applied bias in [17]) was about  $3 \mu\text{m}$ . Thus, in the reverse half-period, the depletion region was viewed as starting deep in the bulk and contracting into  $3 \mu\text{m}$  from the contact with the progression of time. The narrowing of the depletion width with time implied that a lower fraction of positrons were implanted into the depletion region and correspondingly fewer positrons were available to drift back to the interface at longer times, despite the fact that the field strength in the depletion region was still increasing with time. This was found to give a reasonably good representation of the data, although the low-frequency limit predicted by the model was about 7%, deviating slightly from the experimental finding of  $8.5 \pm 0.2\%$  [17].

The difficulty with the interpretation of the peak in  $I_2$  as given in [17] is that the model is in disagreement with present knowledge of the electric field profile at the Au/SI-GaAs contact. The field structure is significantly different from that prescribed by the depletion model. For example, the application of 50 V DC reverse bias causes a field region width of  $\sim 50 \mu\text{m}$  and an approximate constant field strength inside the region of about  $8 \times 10^3 \text{ V cm}^{-1}$  [11]. The measured electric field is about ten times smaller and the measured field region is about 20 times more extensive than those of the depletion approximation. Moreover, under zero-bias conditions, the measured field region extends over  $10 \mu\text{m}$  [11], which is a much larger distance than that expected from the depletion approximation. In the reverse-bias half-period of the AC 50 V bias, it is thus incorrect to suppose that the field region retreats so close to the interface that it penetrates into the positron-sensing region. Therefore, some other explanation for the drop in  $I_2$  at long emission times must be sought.

In order to have a clearer view, the decrease of the electric fields with respect to time is plotted with different timescales in figure 4. At all the temperatures, the electric field decreases



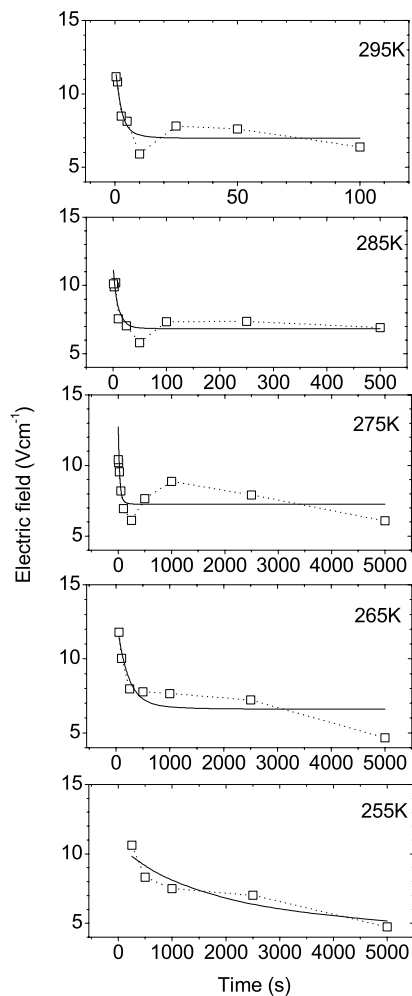


**Figure 4.** Decaying parts of the electric field transients at different temperatures. The transients are plotted with different timescales. The solid curves are the curves modelled by the thermal process neutralizing the space charge region as described in the text. The dashed curves are for visual guidance and long-period damping-like oscillations are clearly observed.

with time after reaching the maximum of about  $10 \text{ kV cm}^{-1}$ , the critical electric field  $E_C$  for the electric field enhancement of EL2 capture [11]. The electric field then drops to about  $7 \text{ kV cm}^{-1}$ , which is the measured field strength of the field region for a DC 50 V reverse bias. Moreover, as seen from figure 4, the time for the electric field decay to the steady-state value is temperature dependent, decreasing with temperature from about 5000 s at 255 K to about 10 s at 295 K. This tends to suggest that apart from the processes of ionization of EL2 and the high-field enhancement of the EL2 capture cross-section which determine the electric field strength close to the contact, there exists another thermally activated process neutralizing the net charge density in the space charge region. We have fitted the decreasing electric field transient data at different temperatures with an exponential decaying term  $\exp(-\lambda t)$ . The fitted curves are plotted in figure 4 and the fitted values of the decay rate  $\lambda$  are shown in figure 5. From figure 5, it can be seen that the decay rate  $\lambda$  follows the general behaviour of a thermal

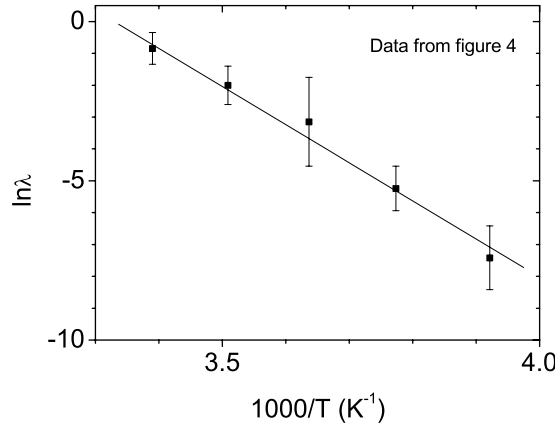


**Figure 5.** A logarithmic plot of the decay rate  $\lambda$  as a function of  $1000/T$ .  $\lambda$  corresponds to the thermally activated physical process which neutralizes the space charge region and thus results in the decay of the electric field. This thermal process is suspected to be related to the recombination of deep-level defect EL5 or EL6.

excitation process having an energy barrier of  $E_b$  (i.e.  $\lambda \sim \exp(-E_b/kT)$ ). The fitted value of this activation energy was found to be  $E_b = 1.03 \pm 0.15$  eV.

#### 4. Discussion

Au *et al* [23] and Tsia *et al* [24] have studied the electric field transient at the AC-biased Au/SI-GaAs contact by monitoring the positron velocity drift caused by the electric field at the contact. In this study, positrons were implanted into a depth of several tens of microns next to the contact and were caused to drift by the electric field. The positron drift velocities were measured by measuring the Doppler shift of the annihilating gamma photons. The present method only probes the  $2 \mu\text{m}$  region next to the contact, while the electric field transient measured by the Doppler shift technique is the mean value weighted with a positron implantation profile which extends over several tens of microns. Apart from this difference, the Doppler shift method requires an electronic feedback system with a time constant of  $\sim 100$  s to keep the annihilation line accurately bisected. This time constant cannot be made much longer, as the feedback system must follow long-term amplification drifts. This limits the longest time for which the electric field transient can be monitored using Doppler shift instrumentation. The method used in the present work is not limited in this way and can monitor very-long-time electric field transients.

In the present study, rather than steadily arriving at the DC value of about  $7 \text{ kV cm}^{-1}$ , the electric field increases with time, reaches the maximum at about  $10 \text{ kV cm}^{-1}$ , and then decreases back to the DC value. The initial increase of the electric field is attributed to electron emission from EL2 and its activation energy was found to be  $0.88 \pm 0.07$  eV. This value is at the limits of the statistical error of the expected value  $0.82$  eV [25]. The slightly high value may arise from systematic effects such as ignoring the electron capture during the electron emission period of EL2. As the measured electric field value reveals the real ionized donor concentration, a discrepancy will occur in the present capture-free model if the capture term contributes significantly during emission. Moreover, the proposed model of the dependence of the electric field's spatial and time dependence in the simple  $E(t)$  expression of equation (6) is provisional and possibly requires more sophistication to give a more exact activation energy. The value of  $d$  is, for example, not perfectly time independent.

The subsequent decrease of the electric field after reaching  $10 \text{ kV cm}^{-1}$  has been shown to be related to a thermally activated process having an activation energy of  $1.03 \pm 0.15 \text{ eV}$  which neutralizes the  $\text{EL2}^+$  charge density. Such a process could be due to either hole emission from an acceptor or neutralization of the space charge region via some recombination centre located at  $1.03 \pm 0.15 \text{ eV}$  above the valence band ( $0.39 \pm 0.15 \text{ eV}$  below the conduction band). In particular, the idea of recombination centre neutralization is a very plausible explanation for the present observation, because the defect energy level obtained statistically coincides with the deep-level defects  $\text{EL5}$  ( $E_C - 0.42 \text{ eV}$ ) and  $\text{EL6}$  ( $E_C - 0.35 \text{ eV}$ ) [25], which are very common in melt-grown GaAs and which have been reported to be recombination centres [26, 27]. If this is the case, this implies that, in addition to the  $\text{EL2}$  deep-level defects, other deep levels, such as  $\text{EL5}$  or  $\text{EL6}$ , also play a significant role in determining the electric field at the SI-GaAs Schottky contact.

Furthermore, if we inspect the decrease of the electric fields at different temperatures (figures 1 and 4) more carefully, in addition to this thermal process having an activation energy of  $1.03 \text{ eV}$ , there is another physical process which makes the electric field oscillate with a much longer timescale. Despite the fact that few data points were taken with relaxation times much longer than the time of the charge neutralization process described in the last paragraph, the electric field transient data taken at 275, 285, and 295 K reach minima, increase, and then decrease again. For the case of 265 K, the electric field shows a decrease with respect to time. The observed  $E_{eff}(t)$  could safely and more accurately be said therefore to be that of a damped harmonic oscillator. However, as also seen from figure 4, the period of oscillation is not constant. Rather, it becomes longer when the system approaches equilibrium. Moreover, the relaxation time of this much slower process varies from of the order of magnitude of  $\sim 100 \text{ s}$  at 295 K to over  $1000 \text{ s}$  at 265 K, which is an abnormally slow process even in a semi-insulating material.

## 5. Conclusions

The positron lifetime technique has been employed to study the average electric field in the  $2 \mu\text{m}$  region next to the Au/SI-GaAs contact in the reverse-bias half-period of a square-wave bias. Studies have been carried out over a range of temperatures and frequencies. It was shown that, by differentiating the measured interfacial intensity as a function of the period, the transient of the electric field close to the contact could be obtained. The electric field was observed to increase with time before reaching the maximum value of  $10 \text{ kV cm}^{-1}$  and then decrease to a value of about  $7 \text{ kV cm}^{-1}$ . The increase of the electric field with respect to time is attributed to the thermal emission from  $\text{EL2}$  and the subsequent build-up of the space charge region. The origin of the subsequent decrease of the electric field is less certain. The present study has, however, revealed that the process is thermally activated. This has led to the speculation that the space charge neutralization is somehow related to the recombination centres  $\text{EL5}$  and/or  $\text{EL6}$ . Moreover, there appears to be an interesting long-timescale oscillating behaviour associated with the  $\text{EL2}^+$  ionization and neutralization. Further study of these unusual phenomena should enable a better understanding of the Au/SI-GaAs system to be achieved.

## Acknowledgments

The work described in this paper was partially supported by grants from the Research Grant Council of the Hong Kong Special Administrative Region, China (under project nos HKU7137/99P and HKU1/00C), HKU CRCG, and the Hung Hing Ying Physical Science research fund.

## References

- [1] Schultz P J and Lynn K G 1988 *Rev. Mod. Phys.* **60** 701
- [2] Puska M J and Nieminen R M 1994 *Rev. Mod. Phys.* **66** 841
- [3] Krause-Rehberg R and Leipner H S 1999 *Positron Annihilation in Semiconductors, Defect Studies (Springer Series in Solid-State Sciences)* (Berlin: Springer) p 127
- [4] Ling C C, Shek Y F, Huang A P, Fung S and Beling C D 1999 *Phys. Rev. B* **59** 5751
- [5] Shek Y F, Ling C C, Fung S and Beling C D 2002 *Appl. Phys. A* **74** 233
- [6] Hu Y F, Ling C C, Beling C D and Fung S 1997 *J. Appl. Phys.* **82** 3891
- [7] Duffy J A, Bauer-Kugelmann W, Kögel G and Trifshäuser W 1997 *Appl. Surf. Sci.* **116** 241
- [8] Asoka-Kumar P, Leung T C, Lynn K G, Nielsen B, Focier M P, Weinberg Z A and Rubloff G W 1992 *J. Appl. Phys.* **71** 5606
- [9] McGregor D S, Rojeski R A, Knoll G F, Terry F L Jr, East J and Eisen Y 1994 *J. Appl. Phys.* **75** 7910
- [10] Berwick K, Brozel M R, Buttar C M, Cowperthwaite M, Sellin P and Hou Y 1994 *Mater. Sci. Eng. B* **28** 485
- [11] Castaldini A, Cavallini A, Polenta L, Canali C, del Papa C and Nava F 1997 *Phys. Rev. B* **56** 9201
- [12] Prints V Ya and Bobylev B A 1981 *Sov. Phys.-Semicond.* **14** 1097
- [13] Prinz V Ya and Rechkunov S N 1983 *Phys. Status Solidi b* **118** 159
- [14] Henry C H and Lang D V 1977 *Phys. Rev. B* **15** 989
- [15] Lang D V and Henry C H 1975 *Phys. Rev. Lett.* **35** 1525
- [16] Rubinger R M, de Oliveira A G, Ribeiro G M, Bezerra J C, Moreira M V B and Chacham H 2000 *J. Appl. Phys.* **88** 6541
- [17] Shan Y Y, Ling C C, Deng A H, Panda B K, Beling C D and Fung S 1997 *Phys. Rev. B* **55** 7624
- [18] Deng A H, Shan Y Y, Fung S and Beling C D 2002 *J. Appl. Phys.* **91** 3931
- [19] Kirkegaard P, Pederson N J and Eldrup M 1988 *PATFIT-88*  
Kirkegaard P, Eldrup M, Morgenson O E and Pederson N J 1981 *Comput. Phys. Commun.* **23** 307
- [20] Brandt W and Paulin R 1977 *Phys. Rev. B* **15** 2511
- [21] Mourino M, Löbl H and Paulin R 1979 *Phys. Lett. A* **71** 106
- [22] Bourgoin J and Lannoo M 1983 *Experimental Aspects (Point Defects in Semiconductors II)* (Berlin: Springer)
- [23] Au H L, Ling C C, Panda P K, Lee T C, Beling C D and Fung S 1994 *Phys. Rev. Lett.* **73** 2732
- [24] Tsia J M, Ling C C, Beling C D and Fung S 2002 *J. Appl. Phys.* **92** 3410
- [25] Martin G M, Mitonneau A and Mircea A 1977 *Electron. Lett.* **13** 191
- [26] Liang Bingwen, Zou Yuanxi, Zhou Bingling and Milnes A G 1987 *J. Electron. Mater.* **16** 177
- [27] Fang Zhao-Qiang, Schiesinger T E and Milnes A G 1987 *J. Appl. Phys.* **61** 5047